THE INFLUENCE OF REINFORCEMENT ON FATIGUE BEHAVIOUR OF A POLYPROPYLENE COMPOSITE

G. Meneghetti[1], M. Ricotta[1*], G. Colombera[2], M. Fusca[1]

[1] *Department of Industrial Engineering, University of Padova, via Venezia 1, 35131 Padova, Italy*
[2] *Electrolux spa , C.so L. Zanussi 30, 33080 Porcia (Pordenone), Italy*
**e-mail: mauro.ricotta@unipd.it*

Keywords: calcium carbonate, fatigue, hysteresis energy, short fibres.

Abstract
In this work the influence of reinforcement (30 wt% 1-mm-long glass fibre, 30 wt% 10-mm-long glass fibre and 42 wt% calcium carbonate) on fatigue behaviour of a polypropylene reinforced composite is investigated. The experimental results show that the high cycle fatigue strength of the polypropylene composite is increased by a factor 3.4 and 2.8 by using 1 mm and 10 mm fibre length, respectively, with respect to 42% calcium carbonate reinforced polypropylene, in terms of applied stress amplitude. However, all experimental results can be synthesised by using the hysteresis energy expended in a unit volume of material per cycle rather than the stress amplitude. Finally the viscoelastic behaviour of 42% calcium carbonate reinforced polypropylene was investigated, showing that the hysteresis energy dissipated in a unit volume of material per cycle due to viscoelasticity is negligible with respect the total plastic strain energy.

1 Introduction

The growing number of applications of short fibre reinforced plastics under cyclic loading in recent years led to an increased interest in understanding their fatigue behaviour. Mandell [1] reviewed a large number of published fatigue studies on short fibre composite materials, considering the effects of the type of matrix and reinforcement, loading parameters (frequency, stress ratio, loading type), as well as environmental parameters and showed that the fatigue strength is increased by increasing the fraction of reinforcement and by using carbon fibre with respect to glass fibre. Mallick et al. [2] analysed the effect of mean stress on the fatigue strength of short 33% by weight E-glass fiber reinforced polyamide-6,6 composite by carrying out tension-tension stress-controlled fatigue tests. They observed that the mean stress has a significant effect on the S-N diagram and they proposed a modified Gerber equation to account for the creep-fatigue interaction at different load ratios. The influence of creep and test frequency on tension-tension fatigue behaviour of 30% by weight glass fiber reinforced polyamide- 6 was noticed also by Bernasconi et al. [3], that proposed a correlation of applied stress with average temperature and strain rate by means of the Larson Miller parameter, allowing for a frequency superposition method based on this parameter. In this paper the influence of reinforcement (30 wt% 1-mm-long glass fibre, 30 wt% 10-mm-long glass fibre and 42 wt% calcium carbonate) on tension-compression fatigue behaviour of polypropylene short fibre composite was investigated and the fatigue data were summarised in a unique scatter band in terms of the hysteresis energy expended in a unit volume of material per cycle, according to energy-based concepts proposed by the authors [4]. Finally

the creep behaviour of 42% by weight calcium carbonate reinforced composite was investigated and it was found that the hysteresis energy dissipated in a unit volume of material per cycle due to viscoelasticity is negligible with respect to the plastic strain energy.

2 Materials and testing methods

The influence of reinforcement on fatigue behaviour of a discontinuous-fibre-reinforced polypropylene was investigated by considering different reinforcements: 30%wt glass fibre with a nominal fibre length of 1 mm (30 GF 1), 30%wt glass fibre with a nominal fibre length of 10 mm (30 GF 10) and 42%wt calcium carbonate. For the latter material two different manufacturing conditions were considered: a first group of specimens (42 CC Type 1) was obtained by cutting the material from a rear tub of a washing machine manufactured by injection moulding and then the coupons were machined to final the geometry shown in Figure 1. Conversely, for a second group of specimens (42 CC Type 2) the same geometry was obtained directly by injection moulding. For each material configuration considered, three static tests were carried-out at room temperature, by imposing a displacement rate equal to 5mm/min, according to ASTM D638 standard [5].

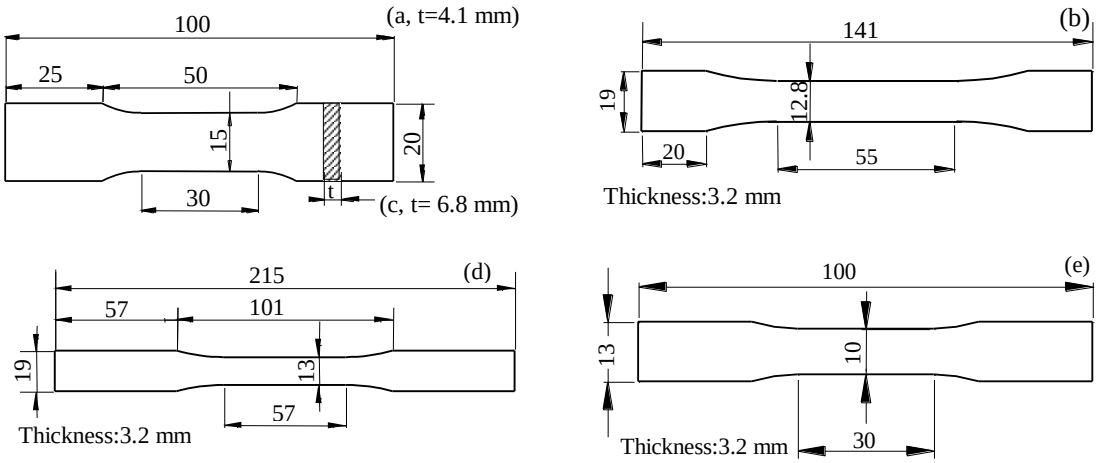

Figure 1. Specimen's geometry adopted for static and fatigue tests: a) 30 GF 10; b) 30 GF 1; c) 42 CC Type 1. For static d) and fatigue e) tests in the case of 42 CC Type 2.

The fatigue tests were carried out by imposing a sinusoidal wave form characterised by a nominal stress ratio R (defined as the ratio between the minimum and the maximum stress) equal to –1. Test frequencies between 1 and 22 Hz were adopted, depending on the applied stress level. In order to maintain the surface temperature of the specimen in the range from 20 to 30° C, a blower was used to cool the samples. The surface temperature of the tested materials was monitored by fixing 0.127 mm diameter copper-constantan thermocouples by means of a silver-loaded conductive epoxy glue. Temperature signals generated by the thermocouples were acquired by means of data logger Agilent Technologies HP 34970A operating at a maximum sample frequency of 22 Hz. During fatigue tests the hysteresis loops were measured by using the signals acquired by the load cell and a MTS extensometer having gauge length of 25 mm. Static and fatigue tests were carried out on specimen's geometry shown in Figure 1. Finally some creep tests were carried-out at room temperature on 42 CC Type 1 specimens by imposing a constant load for 48 hours. After that, in order to evaluate the recovery capacity of the material, the load was removed and the strain was recorded for additional 48 hours by using the same MTS extensometer adopted for fatigue tests. All tests described previously were carried out on a MTS Minibionix servo-hydraulic test machine equipped with a load cell of 15 kN.

3 Static test results

Concerning the static behaviour of the tested materials, Figure 2 shows characteristic engineering stress vs engineering strain curves experimentally measured for each analysed material configuration. It can be seen that the type of reinforcement significantly influences the static behaviour both in terms of ultimate tensile strength σ_{UTS} and strain at fracture ε_{UTS}. Conversely, increasing the fibre length from 1 to 10 mm does not influence significantly σ_{UTS}; on the other hand, ε_{UTS} is halved. The complete separation of the specimen was considered as static failure. It is worth noting that in the case of all specimens made of 42%wt reinforced calcium carbonate the failure condition has never been reached. In fact, due to their high ductility the available stroke of the actuator (100 mm) was not sufficient to separate the specimens. For that, the ε_{UTS} values shown in Figure 2 are not representative of the actual material behaviour. The average values and the standard deviation (st. dv) of elastic modulus E, engineering tensile proof stress $\sigma_{p0.2}$ and engineering tensile strength σ_{UTS} are summarised in Table 1.

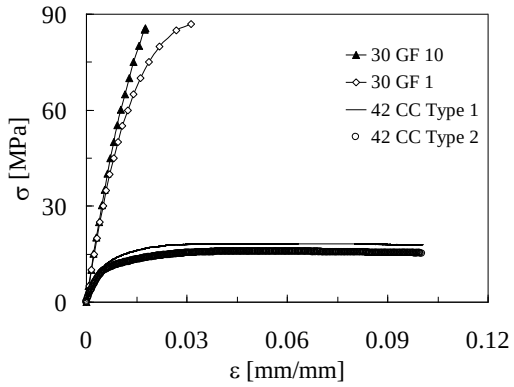

Figure 2. Static stress-strain curves of the tested materials

Material	E [MPa]		$\sigma_{p0.2}$ [MPa]		σ_{UTS} [MPa]		ε_{UTS}	
	Average	St. dv	Average	St. dv	Average	St. dv	Average	St dv
30 GF 1	6690	74	61.1	1.4	87.1	0.6	0.033	0.0015
30 GF 10	6866	215	51.3	1.1	79.0	13.3	0.016	0.0038
42 CC Type 1	3200	59	11.9	1.3	18.6	0.4	-	-
42 CC Type 2	2600	316	10.4	0.9	16.0	0.8	-	-

Table 1. Static mechanical properties of the tested materials

As it is well known, the presence of fibres (independently of their length) increases significantly all static mechanical properties with respect to the PP reinforced by calcium carbonate.

Material	$\sigma_{A,\,50\%}$ [MPa]	$\sigma_{A,\,90\%}$ [MPa]	k	T_σ
30 GF 1	34.8	32.6	22.7	1.13
30 GF 10	28.6	25.5	21.2	1.25
42 CC Type 1	10.3	8.0	11.7	1.65
42 CC Type 2	11.1	9.4	25.2	1.22

Table 2. Fatigue strength data and parameters of the stress-life curve.

In the case of PP reinforced by glass fibres, Table 1 shows an increment of the elastic modulus (2.6%) as well as of the $\sigma_{p0.2}$ (19%) by increasing the fibre length. Conversely, a 9% reduction of the σ_{UTS} was experimentally observed. In the case of 30 GF 10 specimens, it was

observed that the fibres had a preferential orientation. Unfortunately, such preferential orientation was different from one specimen to another, ranging roughly from 20° to 30° with respect to the specimen's longitudinal axis. This explains the large scatter noticed on σ_{UTS} values.

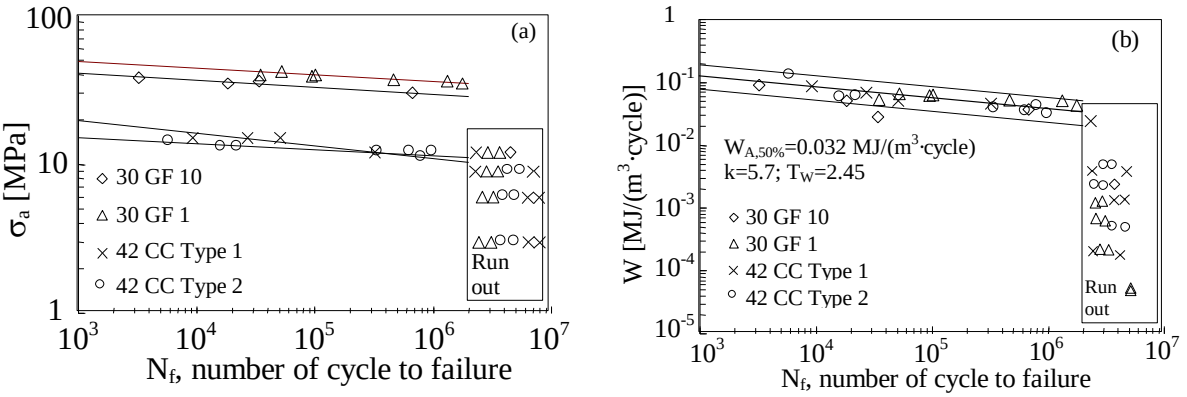

Figure 3. Fatigue test results summarised in terms of a) stress amplitude and b) mechanical energy expended in a unit volume of material per cycle.

4 Fatigue test results

The fatigue data were statistically analysed under the hypothesis of log-normal distribution of the number of cycles to failure. The results of the analysis are summarised in Table 2, where the average fatigue strength at $2 \cdot 10^6$ cycles ($\sigma_{A,\,50\%}$) as well as that referred to a probability of survival of 90% ($\sigma_{A,\,90\%}$) are reported (confidence level 95%). The inverse slope k of the stress-life curves shown in Figure 3a, the scatter index T_σ ($T_\sigma = \sigma_{A,\,10\%} / \sigma_{A,\,90\%}$) are also included. It can be seen that $\sigma_{A,\,50\%}$ is increased by a factor 3.0 and 2.6 with respect to calcium carbonate reinforced polypropylene by using 1-mm- and 10–mm-long fibres, respectively. As noticed in the case of the static behaviour, the increased fibre length does not assure to improve the fatigue strength of the composite material. Finally, a similar fatigue behaviour was found for the two different type of calcium carbonate reinforced composite in the high cycle fatigue regime.

Characteristic hysteresis loops measured during the fatigue tests are shown in Figure 4. Although the nominal stress ratio applied during the fatigue tests was equal to –1, it can be seen that for all tested materials the hysteresis loops shift towards positive mean strains in a continuous manner during the fatigue test, due to the material damage evolution during the fatigue life. Similar results can be found in [6]. The area enclosed within the hysteresis loops represents the mechanical energy expended in a unit volume of material per cycle, W. Figure 5 shows the W trend vs the number of cycles, for all tested materials. One can appreciate that for applied stress amplitude higher than $\sigma_{A,\,50\%}$, the W vs N_f trends do not reach a stabilised value. The opposite behaviour holds true for applied stress amplitude lower than $\sigma_{A,\,50\%}$. Then, by considering the W values measured at 50% of the total fatigue life, the experimental fatigue test results have been processed in terms of specific mechanical energy. It was seen that a unique scatter band having constant slope correlates the fatigue lives in a double logarithmic diagram. Figure 3b shows the results of the statistical analysis under the hypothesis of log-normal distribution of the number of cycles to failure and constant scatter of the experimental data with respect to the mechanical energy level W. Figure 3b reports the mean fatigue curve and those for a survival probability of 10% and 90% with a confidence level of 95%. Each curve has the following expression:

$$W^k \cdot N_f = \text{const} \qquad (1)$$

where N_f is the number of cycles to failure. The figure reports also the inverse slope k of the curves, the mean energy value $W_{A,50\%}$ for the reference fatigue life N_A equal to two million cycles and the energy-based scatter index T_W, defined as $W_{A,10\%}/W_{A,90\%}$. As aforementioned, the test frequency was set in order to maintain the temperature of the material in the range of 20-30° C. To investigate the influence of the test frequency on the fatigue behaviour, during some tests it was varied and the area within the hysteresis loops was analysed. Figure 6a shows as an example the W vs N trend in the case of a 42 CC Type 2 specimen with an applied stress amplitude σ_a=13 MPa and N_f=16390. The specimen was subjected to repeated blocks of cycles and during each block the test frequency was alternatively set to 3 or 22 Hz, until the final failure occurred. It can be seen that, although the test frequency was varied of about seven times, the maximum variation of W was equal to 11%, which was considered negligible from an engineering point of view. Moreover, it was experimentally observed that in fatigue tests at a lower stress amplitude, the influence of test frequency was much lower, i.e. differences smaller than 1% were found.

5. Creep test results

Some creep tests were carried-out on calcium carbonate reinforced PP specimens, since they are more susceptible to creep, due to their lower mechanical properties as compared to those of the glass-fibre reinforced PP. Figure 7a shows the results of creep and recovery tests carried out at three different load levels. It can be seen that strain recovery is not complete. It has been verified that the observed residual strain is comparable with the plastic deformation induced in the material immediately after the creep load is applied. In particular, the 42 CC Type 1 specimen loaded at 10 MPa developed an instantaneous strain ε equal to 0.0032, which implies a plastic deformation equal to $\varepsilon_{pl}=(0.0032-\sigma/E)=(0.0032-10/3940)=6.6\cdot10^{-4}$, that is in good agreement with the residual strain equal to $9.0\cdot10^{-}4$ shown in Figure 7a after recovery. It should be noted that the maximum strain developed during the creep test was about $8\cdot10^{-3}$. In the case of the specimen loaded at 8 MPa, ε was equal to 0.0029 while $\varepsilon_{pl}=(0.0029-8/3500)=6.1\cdot10^{-4}$, which is close to the residual strain equal to $7.9\cdot10^{-4}$, shown again in Figure 7a. Finally, for the sample loaded at 6 MPa, ε was equal to 0.0016 thus $\varepsilon_{pl}=(0.0016-6/4200)=1.7\cdot10^{-4}$, matching the value $1.2\cdot10^{-4}$ observed after recovery. It is worth noting that ε_{pl} was measured by considering the actual elastic modulus of each specimens and not the mean value reported in Table 1. Then, since for all tested specimens it could be verified that the residual deformation after recovery is only due to plastic and not creep strain, the viscoelastic behaviour of material can be described by using a generalised Zener model [7], shown in Figure 7b, where E_R is the relaxed elastic modulus, E_i is the stiffness of *i-th* spring and η_i the viscosity of *i-th* dashpot. Accordingly, the strain vs time during a creep test can be calculated as follows[7]:

$$\varepsilon(t)=\sigma_0/E(t); \quad E(t)=E_R+\sum_{i=1}^{n}E_i\cdot e^{-\frac{t}{\tau_i}} \tag{2}$$

where σ_0 is the constant stress applied during the creep test and $\tau_i=\eta_i/E_i$ is the relaxation time. E_R, E_i, η_i and the number of springs and dashpots are the unknowns of this viscoelastic material model. These parameters have been numerically calculated by means of the least-square method, by considering the experimental total strain minus the plastic component ($\varepsilon-\varepsilon_{pl}$), once the the *i*-parameter is fixed. In this paper it was set *i*=5, as widely suggested in the literature (see [7] as an example). The theoretical creep curves obtained according to generalised Zener model could perfectly fit the experimental ones and then they are not shown in Figure 7a. Moreover it is worth noting that for the 3 different creep load levels, 3 different set of parameters had to be calculated.

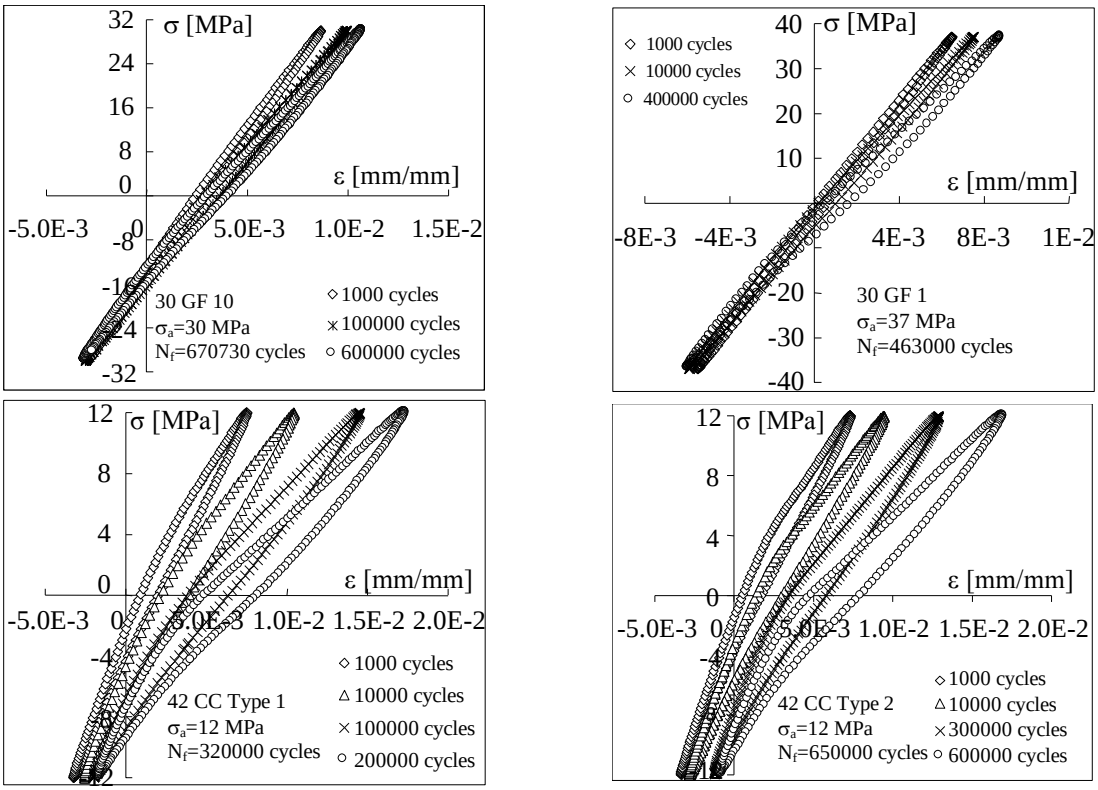

Figure 4. Characteristic hysteresis loops measured during the fatigue tests

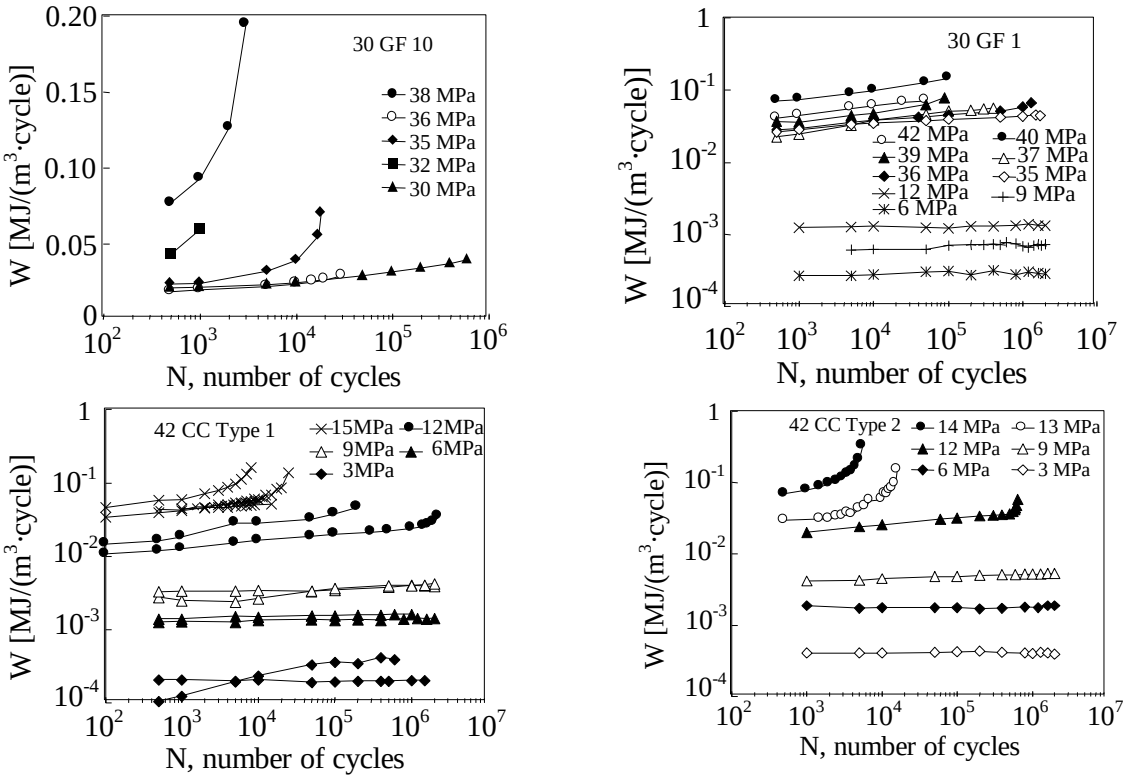

Figure 5. Mechanical energy density per cycle versus the number of cycles for tested materials

Analysing now fatigue loadings, let us consider a sinusoidal stress applied to the generalised Zener model shown in Figure 7b. Due to the viscosity, the stress and the strain waves present a phase shift quantified by the phase angle δ:

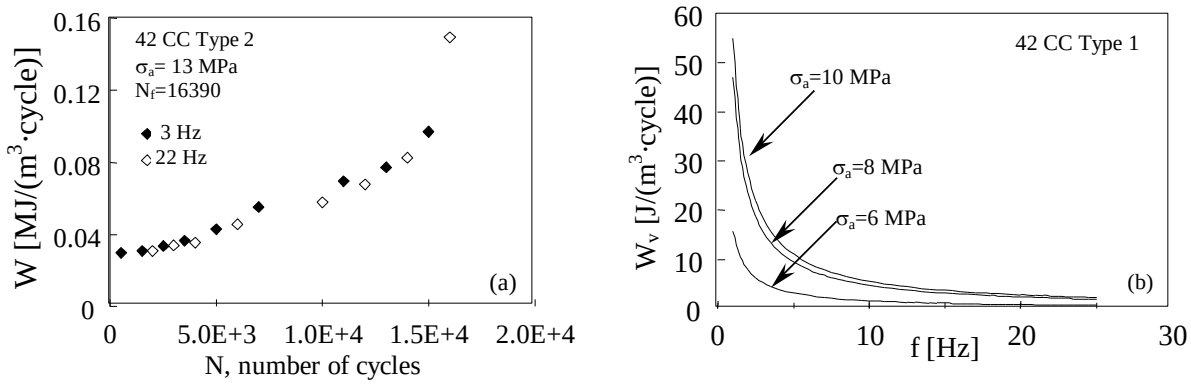

Figure 6. a) Mechanical energy density per cycle vs number of cycles for different test frequencies; b) mechanical energy density per cycle vs test frequency dissipated due to viscosity of material for 42 CC Type

$$\varepsilon(t) = \varepsilon_a \sin(2\cdot\pi\cdot f\cdot t); \qquad \sigma(t) = \sigma_a \sin(2\cdot\pi\cdot f\cdot t + \delta) \tag{3}$$

where f is the test frequency, ε_a and σ_a the strain and stress amplitude. Equations (3) describe an ellipse in the σ-ε plane. The area inside the stress-strain loop is the energy expended in a unit volume of material per cycle W_v, due to its viscoelastic behaviour. The stress can be considered to have two components [7]:

$$\sigma(t) = \sigma_a \sin(2\cdot\pi\cdot f\cdot t)\cos\delta + \sigma_a \cos(2\cdot\pi\cdot f\cdot t)\sin\delta \tag{4}$$

the first of which is in phase with the strain while the second is 90° out of phase. This leads the definition of two dynamic moduli, E' and E'', according to the expressions:

$$E' = \sigma_a \cos\delta/\varepsilon_a; \qquad E'' = \sigma_a \sin\delta/\varepsilon_a \tag{5}$$

which can be combined into a complex modulus E* [7]:

$$E^* = \sigma(t)/\varepsilon(t) = E' + iE'' \tag{6}$$

Then the energy expended to apply creep strains over one period T in a unit volume of material W_v can be calculated:

$$W_v = \int_0^T \sigma d\varepsilon = 2\pi f\varepsilon_a^2 \int_0^T (E'\sin(2\pi f\cdot t)\cos(2\pi f\cdot t) + E''\cos^2(2\pi f\cdot t))dt = \pi\varepsilon_a^2 E'' \tag{7}$$

In the case of generalised Zener model shown in Figure 7b, the dynamic moduli E' and E'' are given by [7]:

$$E' = E_R + \sum_{i=1}^{n} \frac{E_i\cdot(2\pi f)^2\tau_i^2}{1+(2\pi f)^2\tau_i^2}; \qquad E'' = \sum_{i=1}^{n} \frac{E_i\cdot(2\pi f)\tau_i}{1+(2\pi f)^2\tau_i^2}; \tag{8}$$

Figure 6b shows the W_v vs test frequency curves estimated from Eq. (7) and, as expected, it can be seen that there is a significant influence of test frequency on W_v. However, W_v values are three order of magnitude lower than the total mechanical energy W measured during the fatigue tests (see Figure 3b and Figure 5). Then it can be concluded that the total mechanical energy W expended in a fatigue test can be defined as plastic hysteresis energy. On this basis, the substantial independence of W on the test frequency shown in Figure 6a can be justified.

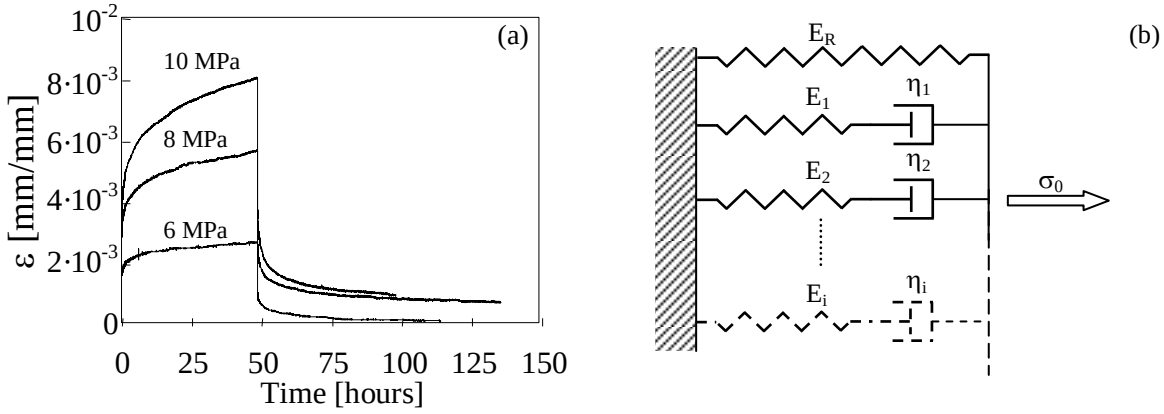

Figure 7. a) creep test results (42 CC Type 1); b) generalised Zener model

6. Conclusions

In this paper the fatigue behaviour under push-pull axial stress of polypropylene reinforced plastic adopted for manufacturing washing machine tubs was investigated. Different types of reinforcement have been considered, namely 30% wt 1-mm-long glass fibr, 30% wt 10-mm-long glass fibre and 42%wt calcium carbonate. The experimental results presented in terms of applied stress amplitude vs number of cycles to failure show that the fatigue strength is highly influenced by the type of reinforcement, being increased by a factor 3.4 and 2.8 by using 1 mm and 10 mm fibre length, respectively, with respect to 42% calcium carbonate reinforced polypropylene. However, the fatigue results can be synthesised in a unique scatter band having a constant slope by using the mechanical energy expended in a unit volume of material per cycle, W, evaluated from the area of the hysteresis loops experimentally measured. The nature of such a mechanical energy was investigated to establish to which extent dissipation is due to plastic rather than creep strains. In view of this, the viscoelastic behaviour of 42%wt calcium carbonate reinforced polypropylene was investigated, being the material most susceptible to creep strains among those tested. After the calibration of a generalised Zener model, the hysteresis energy dissipated in a unit volume of material per cycle W_v due to viscoelasticity was analytically calculated, showing that W_v is three order of magnitude lower than W, in the range of adopted test frequency. Then it is concluded that the expended mechanical energy W is substantially plastic hysteresis energy. Accordingly, the influence of the test frequency on W was found negligible during the fatigue tests.

References

[1] Mandell J.F. *Fatigue behavior of shor fiber composite materials* in "Fatigue of composite materials", edited y Reifsnider K.L. Elsevier, Amsterdam, **4**, pp. 231-337 (1990)
[2] Mallick P.K., Zhou Y. Effect of mean stress-controlled fatigue of a short E-glass fiber reinforced polyamimde-6,6. *International Journal of Fatigue*, **26**, pp. 941-946 (2004).
[3] Bernasconi A., Kulin R.M. Effect of Frequency Upon Fatigue Strength of a Short Glass Fiber Reinforced Polyamide 6: A Superposition Method Based on Cyclic Creep Parameters. *Polymer Composites*, **30**, pp. 154-161 (2009).
[4] Meneghetti G, Analysis of the fatigue strength of a stainless steel based on the energy dissipation. *International Journal of Fatigue*,29, pp. 81-94 (2007).
[5] ASTM D 638-03. Standard test method for tensile properties of plastics (2003).
[6] De Monte M., Moosbrugger E., Quaresimin M. Influence of temperature and thickness on the off-axis behaviour of short glass fibre reinforced polyamide 6.6 – cyclic loading. *Composites: Part A*, **41**, pp. 1368-1379 (2010).
[7] McCrum N.G., Buckley C. P., Bucknall C.B. *Principles of Polymer Engineering*. Oxford Science Publications, Oxford (2007).